CrossMark

ORIGINAL ARTICLE

Histone deacetylase inhibitors deplete myeloid-derived suppressor cells induced by 4T1 mammary tumors in vivo and in vitro

Hai-Fang Wang[1] · Fen Ning[2] · Zong-Cai Liu[3] · Long Wu[4] · Zi-Qian Li[1] · Yi-Fei Qi[1] ·
Ge Zhang[1] · Hong-Sheng Wang[1] · Shao-Hui Cai[4] · Jun Du[1]

Abstract Myeloid-derived suppressor cells (MDSC) have been identified as a population of immature myeloid cells that suppress anti-tumor immunity. MDSC are increased in tumor-bearing hosts; thus, depletion of MDSC may enhance anti-tumor immunity. Histone deacetylase inhibitors (HDACi) are chemical agents that are primarily used against hematologic malignancies. The ability of these agents to modulate anticancer immunity has recently been extensively studied. However, the effect of HDACi on MDSC has remained largely unexplored. In the present study, we provide the first demonstration that HDACi treatment decreases MDSC accumulation in the spleen, blood and tumor bed but increases the proportion of T cells (particularly the frequency of IFN-γ- or perforin-producing CD8+ T cells) in BALB/C mice with 4T1 mammary tumors. In addition, HDACi exposure of bone marrow (BM) cells significantly eliminated the MDSC population induced by GM-CSF or the tumor burden in vitro, which was further demonstrated as functionally important to relieve the inhibitory effect of MDSC-enriched BM cells on T cell proliferation. Mechanistically, HDACi increased the apoptosis of Gr-1+ cells (almost MDSC) compared with that of Gr-1− cells, which was abrogated by the ROS scavenger N-acetylcysteine, suggesting that the HDACi-induced increase in MDSC apoptosis due to increased intracellular ROS might partially account for the observed depletion of MDSC. These findings suggest that the elimination of MDSC using an HDACi may contribute to the overall antitumor properties of these agents, highlighting a novel property of HDACi as potent MDSC-targeting agents, which may be used to enhance the efficacy of immunotherapeutic regimens.

✉ Shao-Hui Cai
  csh5689@sina.com

✉ Jun Du
  dujun@mail.sysu.edu.cn

1 Department of Microbial and Biochemical Pharmacy, School of Pharmaceutical Sciences, Sun Yat-sen University, No. 132 Waihuan East Road, University Town, Guangzhou 510006, People's Republic of China

2 Guangzhou Institute of Pediatrics, Department of Obstetrics, Guangzhou Women and Children's Medical Center, Guangzhou Medical University, Guangzhou, China

3 The Laboratory of Endocrinology and Metabolism, Guangzhou Women and Children's Medical Center, Guangzhou Medical University, Guangzhou, China

4 Department of Pharmacology, School of Pharmaceutical Sciences, Jinan University, Tianhe District, Guangzhou 510632, People's Republic of China

Abbreviations

Arg-1	Arginase-1
BM	Bone marrow
CFSE	Carboxyfluorescein diacetate succinimidyl ester
CTL	Cytotoxic T lymphocyte
DCFH-DA	2′,7′ Dichlorodihydrofluorescein diacetate
GM-CSF	Granulocyte-macrophage colony stimulating factor
HDACi	Histone deacetylase inhibitor(s)
IDO	Indoleamine 2,3-dioxygenase
iNOS	Inducible nitric oxide synthase
iTreg	Inducible regulatory T cell

L-NMMA	L-NG-monomethyl-arginine
MDSC	Myeloid-derived suppressor cell(s)
NaB	Sodium butyrate
NAC	N-Acetylcysteine
nor-NOHA	N^{ω}-Hydroxy-nor-L-arginine
PBMC	Peripheral blood mononuclear cell(s)
ROS	Reactive oxygen species
SAHA	Suberoylanilide hydroxamic acid
SPC	Spleen cell(s)
TCR	T cell receptor

Introduction

Myeloid-derived suppressor cells (MDSC) have been identified as a population of immature myeloid cells that suppress both adaptive and innate anti-tumor immunity in humans and mice [1]. These cells are derived from a myeloid lineage and comprise precursors of macrophages, granulocytes, dendritic cells and myeloid cells [2, 3]. Mouse MDSC are phenotypically characterized by the expression of the cell surface antigens Ly-6C/Ly-6G (both recognized by the Gr-1 antibody) and CD11b, while human MDSC are primarily defined by a CD11b$^+$ CD33$^+$ CD14$^-$ HLA-DR$^-$ phenotype [4]. These cells accumulate in the blood, lymph nodes, bone marrow and tumor beds in many human and animal tumor models [5]. MDSC suppress anti-tumor immunity, primarily by inhibiting the proliferation and activation of T cells, depending on multiple mechanisms, including the expression of inducible nitric oxide synthase (iNOS), arginase-1 (Arg-1) and/or indoleamine 2,3-dioxygenase (IDO) and the production of peroxynitrites and reactive oxygen species (ROS) [2, 6].

Given these immunosuppressive effects, it has been suggested that the elimination of these myeloid suppressor cells may significantly improve anti-tumor responses and enhance the effects of cancer immunotherapy [7, 8]. Many strategies for suppressing the immunosuppressive actions of MDSC have been examined, including treatments designed to favor the differentiation or inhibit the expansion and function of these cells [9, 10]. Several promising results have recently been obtained demonstrating that MDSC can be directly eliminated using certain chemotherapeutic drugs, such as gemcitabine, 5-fluorouracil, docetaxel or doxorubicin [11–14].

Histone deacetylase inhibitors (HDACi), a new generation of chemical agents developed as a therapy primarily against hematologic malignancies, can alter the acetylation of histones in chromatin and enhance the transcription of genes [15]. Almost all HDACi can induce cell cycle arrest, differentiation or apoptosis, by either inducing or repressing relevant gene expression [16]. Among these agents, butyrate [e.g., sodium butyrate (NaB)] was

initially proposed to show anticancer activities, and vorinostat (SAHA) was the first HDACi drug approved by the food and drug administration for clinical use in cancer patients with cutaneous T-cell lymphoma [17]. Extensive evidence suggests that in addition to showing direct tumoricidal activity, HDACi also modulate anti-tumor immunity. HDACi can augment the immunogenicity of tumor cells by upregulating the expression of major histocompatibility complex (MHC) class I and II proteins, co-stimulatory/adhesion molecules (CD40, CD80 and CD86), intercellular adhesion molecule 1 (ICAM1) and MHC class I chain-related molecules (MICA and MICB) on the surface of tumor cells [18, 19]. These effects have been shown to activate IFN-γ-secreting T cell responses and increase CTL-mediated destruction [15, 20].

However, the effects of HDACi on MDSC have remained largely unexplored. In the present study, we investigated the effects of HDACi on the depletion of MDSC and the underlying mechanisms. We provide the first evidence that HDACi treatment decreases MDSC accumulation in the spleen, blood and tumor bed but increases the proportion and activation of T cells in BALB/C mice with 4T1 mammary tumors. In addition, HDACi exposure of bone marrow (BM) cells significantly eliminated the MDSC population induced by GM-CSF or a tumor burden in vitro, which was further demonstrated as functionally important. Mechanistically, the increased apoptosis of Gr-1$^+$ cells (almost MDSC) compared with Gr-1$^-$ cells induced through an increase in intracellular ROS due to HDACi treatment might at least partially account for the observed decrease in the proportion of MDSC.

Materials and methods

Chemicals and reagents

SAHA was purchased from Selleck (Houston, TX, USA) and NaB was obtained from Sigma-Aldrich (St. Louis, MO). Recombinant murine GM-CSF was purchased from Peprotech (Rocky Hill, NJ). Lysis buffer for red blood cells was obtained from Sigma-Aldrich (St. Louis, MO). The iNOS inhibitor L-NG-monomethyl-arginine (L-NMMA) was obtained from Beyotime Biotechnology (Nanjing, China), and the Arg-1 inhibitor (nor-NOHA) was purchased from Cayman Chemical (Ann Arbor, MI). Rat monoclonal anti-Gr-1 (clone RB6-8C5) primary antibody was obtained from Biolegend (San Diego, CA). Antibodies against CD3ε and CD28, and the fluorochrome CFSE used for T cell proliferation assays were obtained from BD Biosciences (Qume Drive San Jose, CA). PE-labeled antibodies against mouse CD11b, CD3, CD4, CD8, FITC-labeled antibodies against mouse Gr-1, CD25, IFN-γ, perforin and

their related isotype controls were obtained from Biolegend (San Diego, CA). APC-labeled antibodies against mouse Foxp3 were obtained from eBioscience. PrimeScript ®RT master mix (Perfect Real Time) and SYBR® Premix Ex TaqTM (Perfect Real Time) were purchased from TaKaRa. EZNA Annexin V and propidium iodide (PI) were obtained from BD biosciences (Qume Drive San Jose, CA).

Animals and cell lines

Six-week-old female BALB/C and C57BL/6 mice were obtained from the Animal Experimental Center of Sun Yat-sen University (Guangzhou, China). The procedures for the handling and care of the mice were approved by the Animal Experimentation Ethics Committee of Sun Yat-sen University (Guangzhou, China). The 4T1 murine mammary tumor cell line was obtained from the Type Culture Collection of the Chinese Academy of Sciences (Shanghai, China). Cells were maintained in RPMI 1640 medium supplemented with 10% fetal bovine serum, 100 μg/ml streptomycin and 100 U/ml penicillin at 37 °C in a humidified atmosphere enriched with 5% CO_2.

Animal models and treatments

To establish the 4T1 mammary tumor mouse model, 1×10^6 4T1 cells were subcutaneously injected into the flank of BALB/C mice to form tumors. At 5 days after tumor cell injection (when the tumor surface area was ~100 mm^2), the mice were intraperitoneally injected with an HDACi (SAHA, 25 or 80 mg/kg), vehicle (2% DMSO, 40% PEG 300, 5% propylene glycol and 1% Tween 80) or normal saline three times a week. Tumor sizes were measured and recorded every 4 days. According to the experimental scheme, the animals were killed on Days 0, 10, 23 and 29 after tumor inoculation, and the spleen, bone marrow, blood and lymph nodes were collected. Cell suspensions of these tissues were subsequently prepared for flow cytometry analysis of the MDSC population or cell culture in vitro. Tumor tissues were further removed and fixed with 4% paraformaldehyde for immunohistochemical examination.

Immunohistochemical examination

Tumor samples isolated from tumor-bearing BALB/C mice were fixed in 4% paraformaldehyde for 24 h prior to processing for immunohistochemical analysis. The procedures were performed according to manufacturer's instructions (Abcam, Cambridge, UK). Briefly, the fixed tumor samples were dissected into small pieces (<3 mm thick), dehydrated, paraffin-embedded and cut into 4-μm-thick sections. The sections were then immunostained with an anti-Gr-1 antibody. Next, high-pressure antigen retrieval was performed using citrate buffer (10 mmol/L, pH 6.0); endogenous peroxidase activity was quenched with 3% hydrogen peroxide in methanol for 15 min, followed by blocking with normal serum for 30 min at room temperature. The sections were subsequently incubated with the primary antibody against Gr-1 (1:500, Biolegend, CA) overnight at 4 °C, followed by incubation with a streptavidin–horseradish peroxidase-conjugated anti-mouse secondary antibody (1:200, Boster, China). Between each step, the sections were washed three times for 10 min with 0.1 M PBS. The sections were subsequently stained using a DAB substrate kit (Boster, China). After washing for 10 min with running water, counter-staining was achieved using hematoxylin. Five random fields of the immunohistochemical sections were observed under a microscope (Nikon, Japan) at a magnification 200×.

MDSC expansion induced by GM-CSF

BM cells were collected from mouse femurs and tibias, then washed twice with PBS and cultured in RPMI 1640 medium supplemented with 10% FBS, 50 μM 2-mercaptoethanol (2-ME). GM-CSF (400 pg/mL) was added to the medium for 2–3 days to stimulate MDSC expansion [21].

Flow cytometry analysis

To label antigens on the cell membrane, cell suspensions from blood, spleen and bone marrow samples obtained from normal and tumor-bearing mice or cultured cells were washed with PBS and subsequently directly incubated with the indicated antibodies (for Gr-1, CD11b, CD3, CD4, CD8, and CD25) or isotype controls (1 h, 4 °C). To label intracellular proteins, the cells were washed, fixed and further permeabilized, and subsequently incubated with the indicated antibodies (perforin, IFN-γ, or Foxp3) or isotype controls. For the detection of apoptosis, BM cells were directly stained with Annexin V and PI without fixation and permeabilization. Subsequently, the cells were washed and resuspended in PBS. For intracellular ROS detection, bone marrow cells were collected and directly stained with oxidation-sensitive fluorescent 2′,7′ dichlorodihydrofluorescein diacetate (DCFH-DA; 5 μM) for 20 min. The fluorescence data were collected using a flow cytometry machine (EXLTM, Beckman Coulter), and the data were analyzed using FlowJo software.

Suppression assays for T cell proliferation

To obtain purified T cells for subsequent T cell proliferation assays, the spleens of naive mice were collected and dissociated into spleen cell suspensions. After red blood

cell lysis, the cell suspensions were incubated in nylon wool columns for 45 min at 37 °C. More than 90% of the eluted cells were confirmed to be T cells after detecting surface CD3 antigens using flow cytometry.

For T cell proliferation assays, spleen T cells were labeled with 1 µM CFSE according to the manufacturer's instructions and plated onto 96-well plates pre-coated with anti-CD3ε and anti-CD28 antibodies.

To examine the effects of HDACi on the inhibitory effect of MDSC-enriched BM cells in T cell proliferation, the same number of living BM cells (containing >70% MDSC) from tumor-bearing mice treated with or without HDACi (SAHA and NaB) was added to the culture (T:BM cells = 4:1 or 2:1). After 3 days, the cells were harvested, and T cell proliferation was determined by measuring the dilution of CFSE using flow cytometry after gating on the $CD3^+$ cell populations.

Quantitative real-time PCR

Total mRNA was extracted from BM cells after treatment. Subsequently, first-strand cDNA synthesis was performed from 500 ng of total RNA. The target and reference genes (β-actin) were quantified in triplicate using the Light-Cycler® 480 II Real-Time PCR System (Roche, Applied Science). The following primers were employed in each reaction: β-actin, forward 5′-CCT GAC CGA GCG TGG CTA CAG C-3′ and reverse 5′-AGC CTC CAG GGC ATC GGA C-3′; Arg-1, forward 5′-AGT CTG GCA GTT GGA AGC AT-3′ and reverse 5′-CAT CTG GGA ACT TTC CTT TC-3′; iNOS, forward 5′-GCT GTT CTC AGC CCA ACA AT-3′ and reverse 5′-TGC AAG TGA AAT CCG ATG TG-3′. After normalization to the β-actin gene, the expression levels of each target gene were calculated using the comparative threshold cycle (CT) method. Δct values were calculated according to the formula Δct = ct (gene of interest) − ct (β-actin), and $2^{-\Delta\Delta ct}$ was calculated, where ΔΔct = Δct (control group) − Δct (experimental group), for the determination of expression, expressed as the fold change between the experimental and control samples.

Statistical analysis

Results were expressed as mean ± standard deviation (SD) of three independent experiments unless otherwise specified. Student's *t* test and one-way ANOVA were performed to compare the differences between groups. Statistical analyses were performed using GraphPad Prism Software version 5.0 (GraphPad Software Inc., La Jolla, CA). $P < 0.05$ was considered as statistically significant.

Results

Direct depletion of MDSC by HDACi (SAHA) treatment decreases MDSC accumulation in mice with 4T1 mammary tumors

To study the effect of HDACi on MDSC expansion, a frequently used animal model was established to induce MDSC expansion. In this model, mice were injected with 4T1 mammary tumor cells to form tumors, and dramatic expansion of MDSC ($CD11b^+$/$Gr-1^+$) was observed in the spleen, blood and bone marrow during tumor growth (Supplementary Fig. 1). In this model, SAHA was intraperitoneally administered at two doses (25 and 80 mg/kg) to study the effect of HDACi treatment on MDSC expansion in vivo. The results shown in Fig. 1b demonstrated that SAHA treatment did not markedly change the tumor volume prior to Day 17 but reduced the tumor volume thereafter compared with the controls. We observed that the tumor volume was significantly decreased in mice after SAHA treatment compared with that of the controls at Day 29, as shown in the lower panels in Fig. 1b. These results confirmed the direct anti-tumor properties of SAHA, as described in earlier reports. Previous studies have shown that lower tumor burdens stimulate less MDSC accumulation than larger tumor burdens in mice, suggesting that a reduced tumor burden induced by the toxicity of an HDACi might indirectly decrease MDSC accumulation. To objectively determine the direct effect of SAHA on MDSC expansion, samples were collected on Day 23 and, especially, on Day 10 (when the mice exhibited comparable tumor burdens) and analyzed via flow cytometry (Fig. 1b). The results revealed that SAHA treatment at the indicated two doses significantly decreased the proportion of MDSC in the spleen but only slightly decreased the proportion of MDSC in peripheral blood on both Days 10 and 23 compared with the controls (Fig. 1c). Furthermore, using an immunohistochemical staining approach, we observed that the number of $Gr-1^+$ cells in the tumor bed was diminished after SAHA administration compared with the number in the untreated group on Day 10 (Fig. 1d). These results collectively demonstrated that the direct depletion of MDSC through HDACi (SAHA) treatment contributes to the decrease in MDSC accumulation in mice with 4T1 mammary tumors.

HDACi (SAHA) treatment increases the proportion and activation of T cells in BALB/C mice with 4T1 mammary tumors

Increased MDSC infiltration in the tumor bed was associated with a reduction of anti-tumoral effector T cells
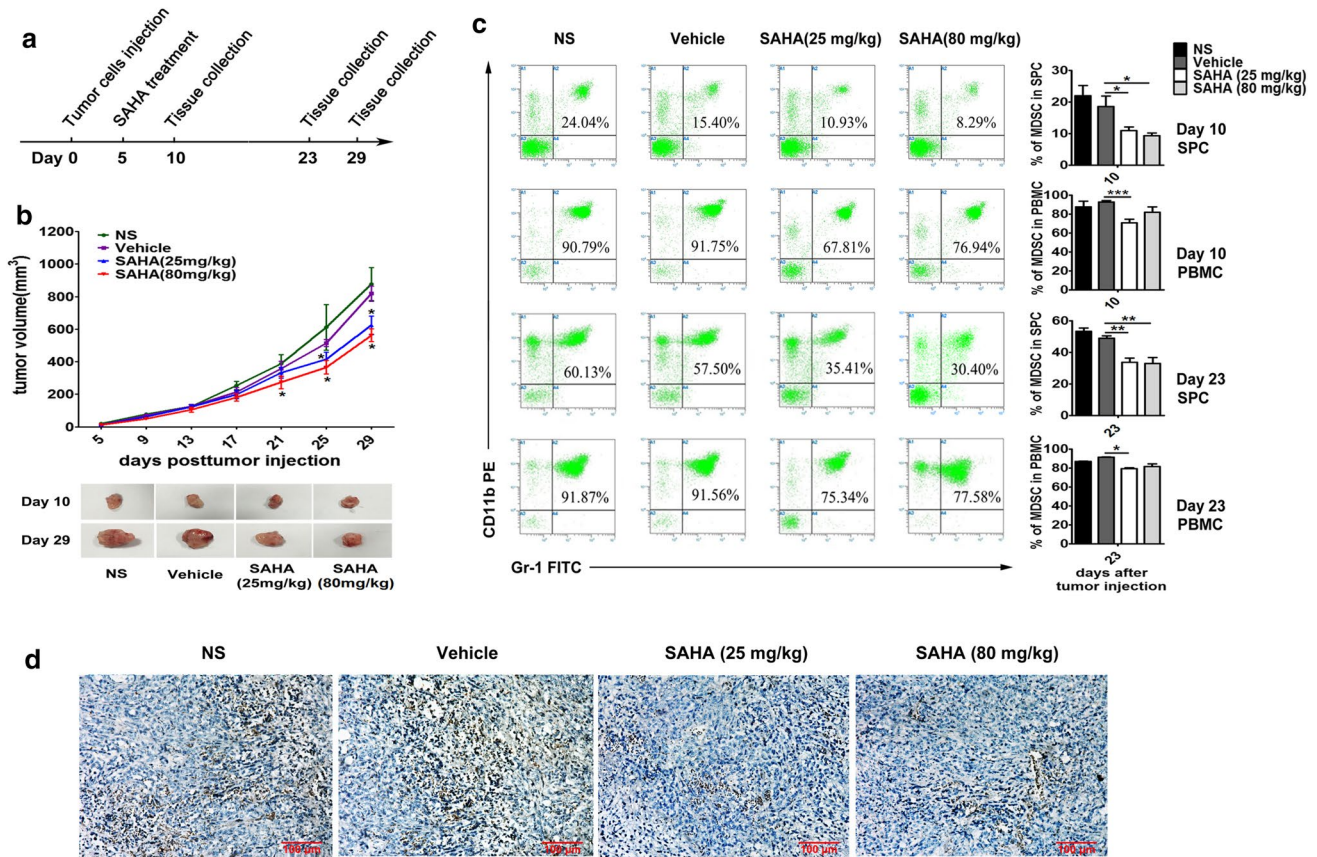
Fig. 1 HDACi (SAHA) eliminates MDSC induced by 4T1 mammary tumors in BALB/C mice. **a** Schematic representation of the experimental design for evaluating the effect of an HDACi (SAHA) on MDSC induced by 4T1 tumors. A total of 1×10^6 4T1 cells were subcutaneously injected into the flank of BALB/C mice to generate tumors. On Day 5, the mice were intraperitoneally injected with SAHA (25 or 80 mg/kg), vehicle or NS three times a week. **b** The tumor volume was measured and recorded every 4 days after SAHA treatment (*upper curve graph*). Representative tumor images show the changes in volume between the groups on Days 10 and 29 (*lower images*). **c** Spleen and blood cells were collected and labeled with fluorescently labeled monoclonal antibodies to analyze the proportion of MDSC (Gr-1$^+$/CD11b$^+$) among these cells using flow cytometry on Days 10 and 23 (*left*). The average percentages of MDSC in the spleen and PBMC of different treatment groups were further calculated on Days 10 and 23 and are displayed in histograms (*right*). **d** Tumor samples isolated from BALB/C mice were collected and fixed for immunohistochemical analysis on Day 10. Tumor sections were immunostained to label Gr-1$^+$ cells in the tumor beds from different groups. Representative images are shown at a ×200 magnification. *Scale bar* 100 µm. *$P \leq 0.05$, **$P \leq 0.01$, ***$P \leq 0.001$; $n = 5$ mice per group

during tumor progression. Thus, we next sought to determine whether the depletion of MDSC through HDACi (SAHA) treatment enhanced the immune response by altering the proportion or activation of T cells. Interestingly, the results showed that the frequency of CD4$^+$ and CD8$^+$ T cells in the spleen was significantly increased after SAHA administration (Fig. 2a). Furthermore, the percentage of IFN-γ-producing CD8$^+$ T cells, but not CD4$^+$ T cells, was significantly elevated after SAHA treatment compared with the percentage in the controls (Fig. 2b). In addition, SAHA treatment markedly increased the frequency of perforin-producing CD8$^+$ T cells (Fig. 2c). Taken together, these results demonstrated that HDACi (SAHA) treatment increased the proportion and activation of T cells in BALB/C mice with 4T1 mammary tumors.

HDACi (SAHA and NaB) exposure significantly depletes MDSC induced by GM-CSF in BM cells or a tumor burden in vitro

Considering the depletion of MDSC in vivo, we reasoned that HDACi might exhibit the same effect in vitro. However, there is limited information concerning the drug distribution of SAHA and NaB in the organ compartments of mice. Thus, the dose of an HDACi to which bone marrow would typically be exposed in a therapeutic setting is unclear. It was previously reported that after a single oral dose (50 mg/kg) of SAHA, the maximum concentration of SAHA detected in mouse plasma was approximately 2 µM, and when NaB was orally delivered to mice at 5 g/kg, the peak plasma butyrate concentrations was approximately

Fig. 2 HDACi (SAHA) increases the proportion and activation of T cells in BALB/C mice with 4T1 tumors. The 4T1 tumor-bearing animals were treated as indicated, and their spleen cells were isolated on Day 10 and subjected to subsequent flow cytometry detection. **a** Changes in the frequency of CD4⁺ and CD8⁺ T cells in spleen cells after SAHA (25 or 80 mg/kg) treatment. **b** Changes in the percentage of IFN-γ-producing CD4⁺ or CD8⁺ T cells in spleen cells after SAHA treatment. **c** Changes in the percentage of perforin-producing CD8⁺ T cells in spleen cells after SAHA treatment. *P ≤ 0.05; n = 5 mice per group
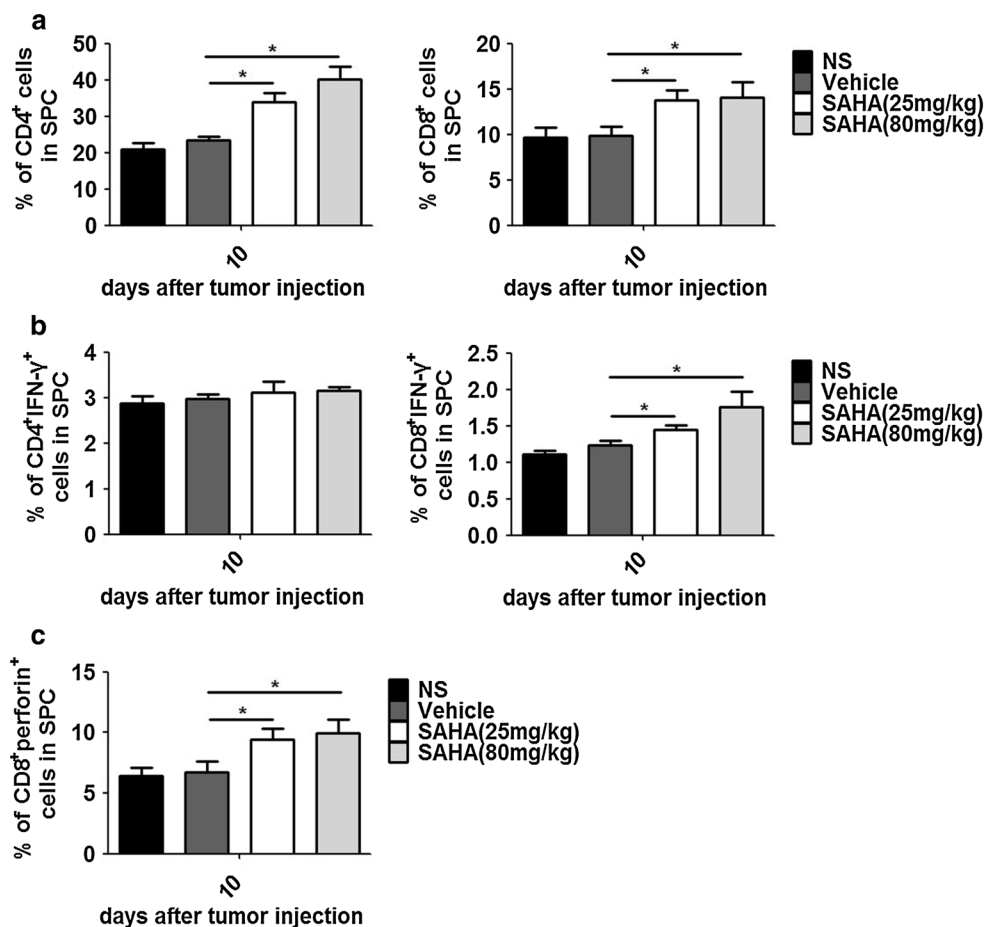
9 mM [22, 23]. According to this information, combined with our previous findings [24, 25] and preliminary analyses (Supplementary Figs. 3 and 4), we selected HDACi concentrations of 2 μM for SAHA and 2.4 mM for NaB to be used in in vitro experiments with BM cells in the present study. We examined the direct toxicity of SAHA and NaB to BM cells at doses ranging from 0.25 to 2.5 μM and 0.3 to 3 mM, respectively, in preliminary analyses. The results showed that both SAHA and NaB exhibited increasing toxicity at increasing concentrations. However, after SAHA and NaB treatment at doses of 2 μM and 2.4 mM, respectively, for 24 h, approximately 40% of the BM cells from tumor-bearing mice survived, which was sufficient for the in vitro experiments (Supplementary Fig. 3).

To study the effects of HDACi on MDSC expansion in vitro, GM-CSF (400 pg/ml) was used to induce MDSC expansion in vitro, and the proportion of MDSC in BM cells was observed to be dramatically increased after GM-CSF stimulation for 72 h (Fig. 3a). Importantly, the proportion of MDSC among the residual living BM cells was decreased to an undetectable level after SAHA or NaB treatment (Fig. 3a). Notably, the proportion of MDSC in the control group was also decreased to an undetectable

level after SAHA or NaB treatment (Fig. 3a). Furthermore, isolated murine BM cells containing >70% MDSC induced under a tumor burden were also used to determine the effects of HDACi treatment on MDSC in vitro. The results showed that the proportion of MDSC among the residual living BM cells was also decreased to an undetectable level after SAHA or NaB treatment (Fig. 3b). These findings collectively demonstrated that HDACi (SAHA and NaB) exposure significantly depleted MDSC in BM cells induced by GM-CSF or a tumor burden in vitro.

MDSC-enriched BM cells from tumor-bearing mice fail to inhibit T cell proliferation after HDACi treatment

MDSC suppress the proliferation of T cells [8]. If the HDACi-induced depletion of MDSC in BM cells is functionally important, then equal numbers of BM cells from 4T1 tumor-bearing mice should be more suppressive than equal numbers of BM cells from tumor-bearing mice pretreated with HDACi (SAHA and NaB) in vitro. The effect of residual living BM cells after treatment with or without HDACi (SAHA and NaB) on the proliferation of T cells was therefore tested using a well-described T cell receptor
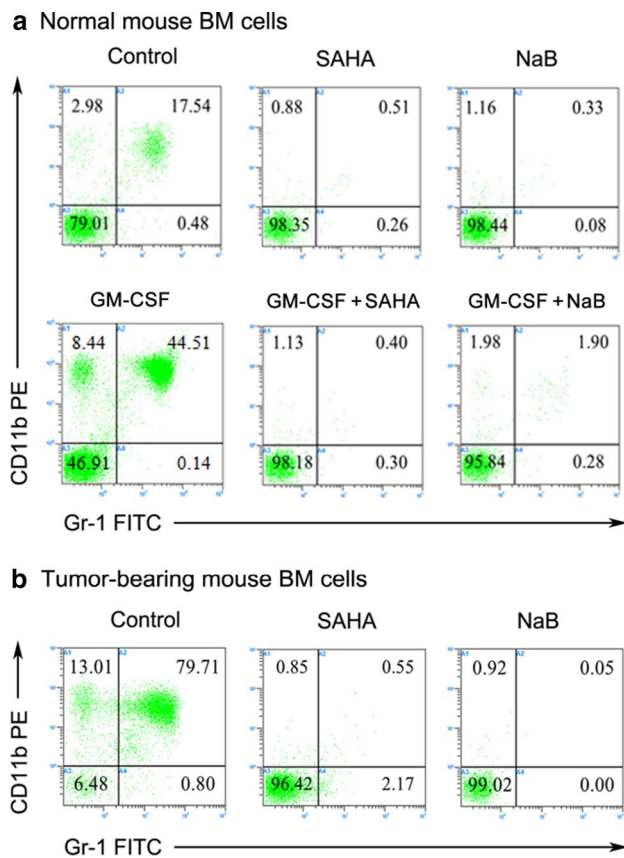
a Normal mouse BM cells

b Tumor-bearing mouse BM cells

Fig. 3 HDACi (SAHA and NaB) exposure significantly depletes MDSC induced in BM cells by GM-CSF or a tumor burden in vitro. **a** Normal mouse BM cells were collected and pre-cultured with or without GM-CSF (400 pg/ml) for 3 days and further treated with or without SAHA (2 μM) and NaB (2.4 mM) for an additional 24 h. Subsequently, the percentage of MDSC in BM cells was detected using flow cytometry. **b** BM cells collected from tumor-bearing mice were treated with or without SAHA (2 μM) and NaB (2.4 mM) for 24 h. Subsequently, the percentage of MDSC in BM cells was detected using flow cytometry. The data represent one of the three experiments that were independently performed and analyzed

(TCR)-activated T cell proliferation assay. The results demonstrated that induced T cell proliferation was indeed suppressed after co-culture with BM cells derived from tumor-bearing mice (containing >70% MDSC) at two different ratios (T:BM cells = 4:1 or 2:1). Furthermore, this immunosuppressive activity was almost completely abolished after HDACi (SAHA and NaB) pre-treatment of BM cells (Fig. 4a). As previously described, Arg-1 and iNOS are two critical mediators that play immunosuppressive roles in MDSC. Thus, if the MDSC population in MDSC-enriched BM cells plays the predominant immunosuppressive role, then immunosuppression should be at least partially abrogated by Arg-1 and iNOS inhibitors. As expected, the immunosuppression effect was largely abrogated by treatment with either the Arg-1 inhibitor nor-NOHA or the iNOS inhibitor L-NMMA (Fig. 4b), indirectly suggesting

that the MDSC population in BM cells played the predominant immunosuppressive role. In addition, we confirmed that the gene expression of Arg-1 and iNOS in MDSC-enriched BM cells was significantly decreased after MDSC depletion due to SAHA and NaB treatment (Fig. 4c). Taken together, these data suggested that HDACi (SAHA and NaB)-induced MDSC depletion is functionally important.

HDACi treatment induces a 2-fold increase in the apoptosis of Gr-1$^+$ cells compared with Gr-1$^-$ cells through increasing intracellular ROS in BM cells

Previous studies have shown that chemotherapeutic drugs, such as doxorubicin and 5-fluorouracil, result in depletion of MDSC through the selective apoptosis of these cells. We therefore speculated that the significant depletion of MDSC induced by HDACi (SAHA and NaB) might also reflect the selective killing of MDSC. Interestingly, the results demonstrated that SAHA (2 μM) and NaB (2.4 mM) induced approximately 2-fold more apoptosis of Gr-1$^+$ cells compared with Gr-1$^-$ cells in BM cells from tumor-bearing mice in vitro (Fig. 5a). These data indicated that HDACi (SAHA and NaB) might induce more, rather than selective, MDSC apoptosis. Based on these results, we reasoned that more apoptosis would be induced by HDACi treatment in BM cells from 4T1 tumor-bearing mice than in an equal number of BM cells from normal mice. As expected, the results showed that SAHA (4 μM) and NaB (5 mM) induced more apoptosis of BM cells from 4T1 tumor-bearing mice compared with those from normal mice (Fig. 5b). As previously described, HDACi trigger apoptosis by elevating ROS levels [26, 27]; thus, we speculated that HDACi might enhance the increase in ROS production in MDSC, leading to ROS-dependent apoptosis. First, we assessed whether HDACi treatment increases intracellular ROS levels in BM cells. The results showed that SAHA (2 μM) and NaB (2.4 mM) treatment significantly increased intracellular ROS levels in BM cells (Fig. 5c). Subsequently, N-acetylcysteine (NAC), which eliminates intracellular ROS, was used to determine whether the induction of ROS production by HDACi treatment functions as a potential mechanism for the enhanced apoptosis of Gr-1$^+$ cells using flow cytometry. The results showed that the enhancement of apoptosis in Gr-1$^+$ cells induced by the HDACi was largely reversed after the addition of NAC (Fig. 5d). These findings collectively demonstrated that HDACi induced more apoptosis of Gr-1$^+$ cells than Gr-1$^-$ cells through increasing intracellular ROS in BM cells.

Discussion

MDSC, a primary suppressive cell population, have been widely documented in animals and patients with tumors.
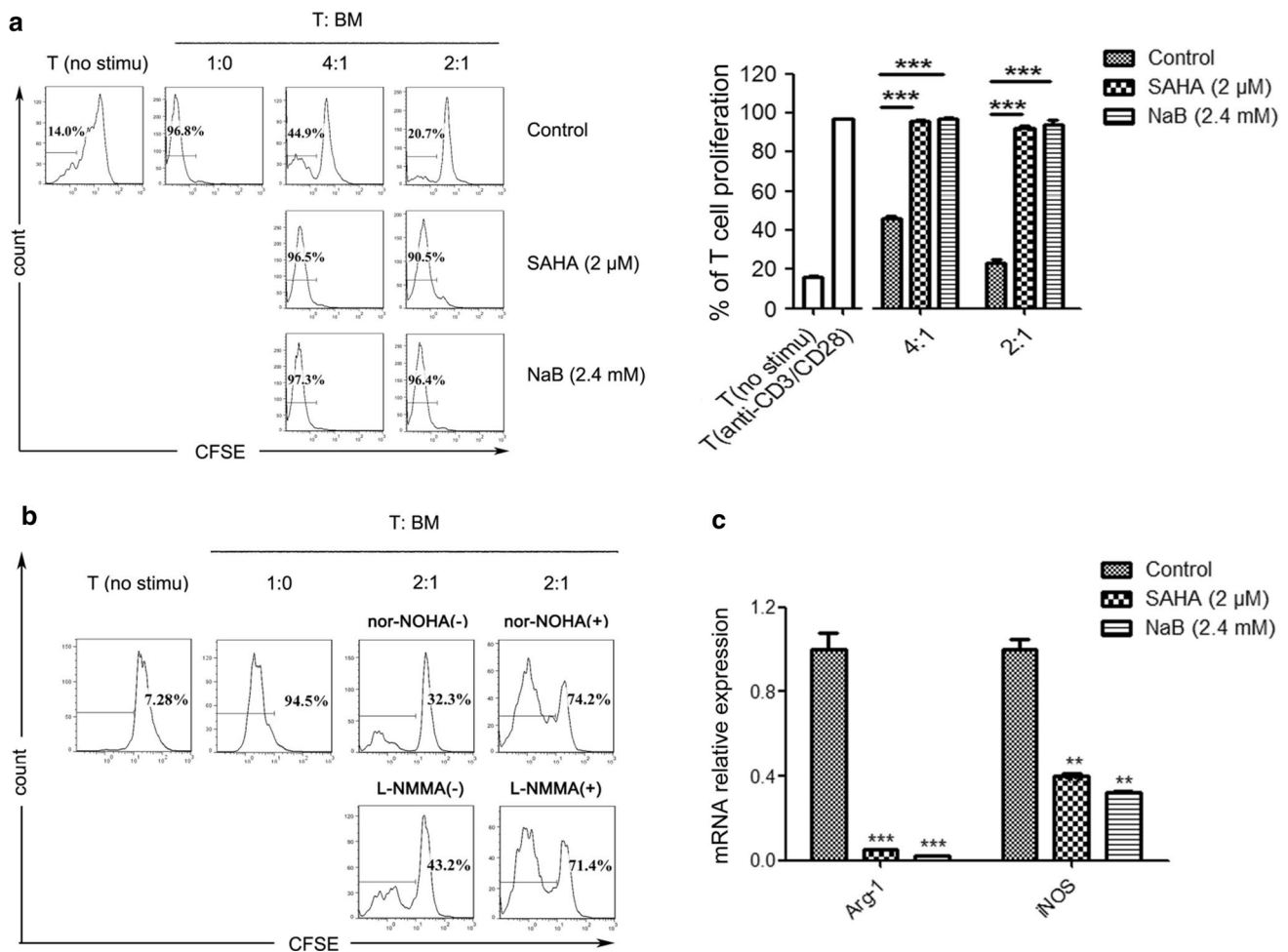
Fig. 4 BM cells from tumor-bearing mice failed to inhibit T cell proliferation after HDACi treatment. A T cell proliferation suppression assay was performed to investigate the effects of HDACi on the activity of BM cells derived from tumor-bearing mice (containing >70% MDSC) in inhibiting T cell proliferation. **a** BM cells from tumor-bearing mice were treated with or without SAHA (2 µM) and NaB (2.4 mM) for 24 h and subsequently harvested and used to inhibit T cell proliferation at different ratios (T:BM cell = 4:1 or 2:1). After three days, the mixed cells were harvested, and T cell proliferation was determined by measuring the dilution of CFSE using flow cytom-

etry after gating on the $CD3^+$ cell populations. Flow cytometry data (*left*) and histograms (*right*) are shown. **b** Nor-NOHA (Arg-1 inhibitor) and L-NMMA (iNOS inhibitor) were used to study the roles of Arg-1 and iNOS in the inhibition of T cell proliferation induced by MDSC-enriched BM cells. **c** BM cells from tumor-bearing mice were treated with or without SAHA (2 µM) and NaB (2.4 mM) for 12 h, and the relative mRNA expression of Arg-1 and iNOS was analyzed using qRT-PCR. **P ≤ 0.01, ***P ≤ 0.001. The data represent one of the three experiments that were independently performed and analyzed

The elimination of MDSC may significantly improve anti-tumor responses and enhance the effects of cancer immunotherapy. Accordingly, depletion of Gr-1+ MDSC using an anti-Gr-1 monoclonal antibody restores T-cell antitumor activity [28, 29]. However, anti-Gr-1 also depletes all mature granulocytes, leading to severe immunosuppression [8]. The promotion of MDSC differentiation using all-trans retinoic acid (ATRA), a natural metabolite of vitamin A, has also been considered [30]. Recent studies have revealed that several cytotoxic agents, such as gemcitabine, 5-fluorouracil and doxorubicin, not only exert a direct cytotoxic effect on tumor cells but also eliminate MDSC in vivo in mice and humans [13, 31]. In the present study, we provide

the first evidence that HDACi eliminates MDSC in vivo and in vitro. Using a 4T1 tumor-bearing mouse model, we demonstrated that HDACi (SAHA) administration reduced the proportion of MDSC in the spleen, blood and tumor beds. The results also showed that the inhibitory effect of SAHA was more obvious in the spleen than in blood, and there was no significant difference between the two doses of SAHA used. Rosborough et al. previously reported that the HDACi reagent TSA facilitates, rather than inhibits, the GM-CSF-mediated expansion of MDSC in vitro and in vivo; these authors also demonstrated that SAHA promotes GM-CSF-stimulated MDSC expansion in BM cell cultures, contradictory to the findings presented herein
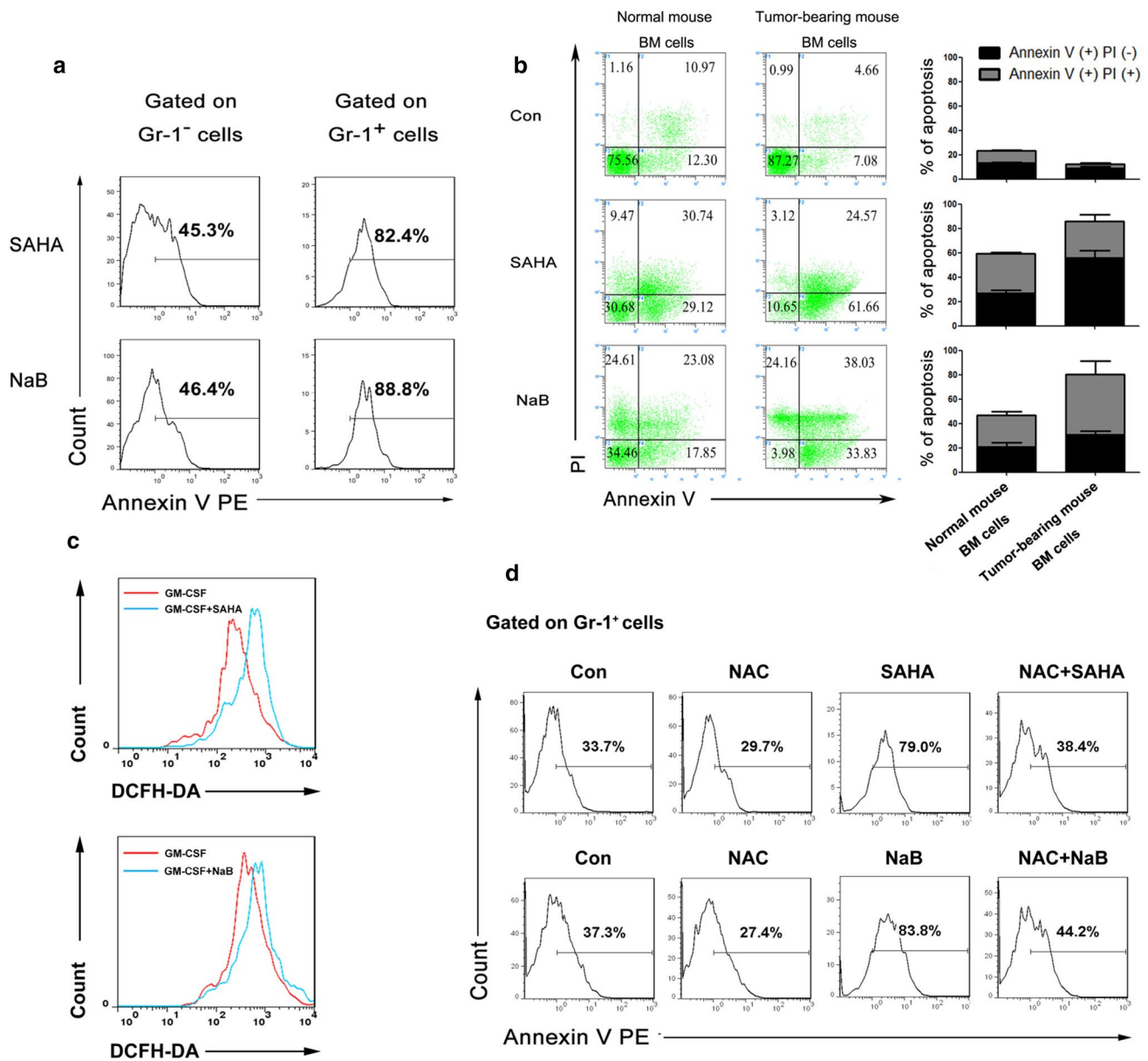
Fig. 5 HDACi (SAHA and NaB) induces a greater increase in the apoptosis of Gr-1$^+$ than Gr-1$^-$ cells through increasing intracellular ROS. **a** BM cells from tumor-bearing mice were treated with or without SAHA (2 µM) and NaB (2.4 mM) for 24 h, and the cells were subsequently stained with an anti-Gr-1 antibody and Annexin V to detect the differences in cell apoptosis between Gr-1$^+$ and Gr-1$^-$ BM cells using flow cytometry. **b** BM cells from normal mice and tumor-bearing mice were treated with or without SAHA (4 µM) and NaB (5 mM) for 24 h, and the cells were stained with Annexin V and PI. Subsequently, the percentage of apoptotic cells was analyzed using flow cytometry, and the average percentage of apoptotic cells (Annexin V$^+$/PI$^-$ and Annexin V$^+$/PI$^+$) was further calculated, as shown in the histogram. **c** BM cells from normal mice were pre-treated with or without GM-CSF (400 pg/ml) for 3 days, followed by co-treatment with or without SAHA (2 µM) and NaB (2.4 mM) for an additional 8 h. BM cells were subsequently incubated with DCFH-DA for intracellular ROS detection through flow cytometry. Representative flow cytometry data showing the changes in the intracellular ROS level in BM cells after SAHA and NaB treatment are presented. **d** BM cells from tumor-bearing mice were pre-treated with or without N-acetylcysteine (NAC) for 12 h, followed by co-treatment with or without SAHA (2 µM) and NaB (2.4 mM) for an additional 24 h. Subsequently, the cells were stained with an anti-Gr-1 antibody and Annexin V to detect differences in cell apoptosis between Gr-1$^+$ cells under different treatments using flow cytometry. The data represent one of the three experiments that were independently performed and analyzed

[32]. However, this previous study was conducted using relatively lower concentrations (0.1–10 nM for TSA and 10–500 nM for SAHA) than were used in the present study.

Interestingly, the data presented in Supplementary Fig. 4 confirmed that SAHA and NaB increased the proportion of MDSC at lower doses of 0.25–0.5 µM and 0.3–0.6 mM,

respectively. However, at higher doses of 1–2 µM and 1.2–2.4 mM, treatment with SAHA and NaB, respectively, started to deplete MDSC. This result suggested that HDACi might promote MDSC expansion at relatively lower doses and prevent expansion at more therapeutically relevant doses.

Increased MDSC infiltration in tumor beds is associated with a reduction of activated anti-tumoral T cells during tumor progression [8]. Thus, we examined whether the depletion of MDSC by HDACi (SAHA) treatment may influence the proportion or activation of T cells in vivo. Interestingly, the frequency of CD4$^+$ and CD8$^+$ T cells in the spleen was significantly increased, and the percentage of IFN-γ- and perforin-producing CD8$^+$ T cells, rather than CD4$^+$ T cells, was also significantly elevated after SAHA administration. In addition, the proportion and absolute number of iTregs (CD4$^+$CD25$^+$FoxP3$^+$) in the lymph nodes was markedly decreased after SAHA treatment (Supplementary Fig. 2). These results indicated that an HDACi (SAHA) might improve the immune responses of T cells through depletion of MDSC in BALB/C mice with 4T1 mammary tumors.

We further investigated the effects of HDACi (SAHA and NaB) on MDSC in vitro and observed that the accumulated MDSC population in BM cells induced by either GM-CSF or a tumor burden was eliminated to an undetectable level after exposure to an HDACi (2 µM SAHA or 2.4 mM NaB) in vitro. We further observed that the HDACi-induced depletion of MDSC was more complete in vitro than in vivo. We speculated that this observation might reflect the consecutive renewal of MDSC induced by tumor-derived factors through the stimulation of myelopoiesis, inhibition of immature myeloid cell differentiation and potentially different cytotoxicity to MDSC in vivo and in vitro. Furthermore, we demonstrated that the HDACi-induced elimination of MDSC in BM cell populations was functionally important. The results confirmed that BM cells from tumor-bearing mice (containing >70% MDSC) significantly suppressed the proliferation of T cells, and pre-treatment with an HDACi (SAHA or NaB) almost fully abrogated this suppression. Arg-1 and iNOS are two well-known mediators of the immunosuppressive activity of MDSC [33]. Arginase metabolizes the substrate L-arginine, resulting in a shortage of L-arginine in the microenvironment and inhibition of T-cell proliferation, while iNOS metabolizes L-arginine and generates NO to suppress T-cell function [1]. Importantly, we observed that the suppression of T cell proliferation induced by MDSC-enriched BM cells was largely abrogated by an inhibitor of either Arg-1 (nor-NOHA) or iNOS (L-NMMA), demonstrating the predominant role of the MDSC population in BM cells from tumor-bearing mice. Furthermore, we demonstrated that the gene expression of both Arg-1 and iNOS was significantly decreased in MDSC-enriched BM cells after HDACi (SAHA and NaB) treatment in vitro, and we speculated that this effect might result from the depletion of MDSC, rather than the direct suppression of gene expression by HDACi in BM cells. These data collectively suggest that HDACi treatment abolishes the immunosuppressive action of MDSC and can potentially be employed as an immunotherapeutic regimen.

As previously described, chemotherapeutical drugs eliminate MDSC in tumor-bearing mice through different putative mechanisms. Gemcitabine, 5-fluorouracil and doxorubicin induce the selective apoptosis of MDSC. The selective effect of 5-fluorouracil reflects the decreased expression of thymidylate synthase in MDSC [14]. The selective effect of doxorubicin partially reflects enhancement of the high production of ROS by MDSC (compared with other cell subsets), leading to ROS-dependent apoptosis [12]. However, the related mechanism for gemcitabine remains unexplored. We initially speculated that the depletion of MDSC by HDACi treatment might reflect the selective killing of MDSC. However, the results showed that SAHA (2 µM) and NaB (2.4 mM) induced approximately 2-fold more apoptosis in Gr-1$^+$ cells than in Gr-1$^-$ cells in vitro, indicating that HDACi might trigger more, rather than selective, apoptosis of MDSC. This finding suggested that the greater HDACi-induced increase in the apoptosis of Gr-1$^+$ cells compared with Gr-1$^-$ cells might at least partially account for the decreased MDSC population. Regarding the mechanism underlying how HDACi induce increased apoptosis of Gr-1$^+$ cells, we speculated that HDACi might enhance the high production of ROS in MDSC such as doxorubicin, leading to ROS-dependent apoptosis, as HDACi trigger apoptosis by elevating ROS levels [26, 27]. As speculated, SAHA and NaB treatment significantly increased intracellular ROS levels in BM cells. More importantly, the enhancement of apoptosis in Gr-1$^+$ cells induced by HDACi was largely reversed after the addition of NAC. These findings collectively indicated that the HDACi induced a greater increase in the apoptosis of Gr-1$^+$ cells compared with that of Gr-1$^-$ cells through increasing intracellular ROS in MDSC-enriched BM cells.

Notably, the depletion of MDSC to undetectable levels in vitro may not be fully explained by the HDACi-induced increase in the apoptosis of Gr-1$^+$ cells. Chemotherapeutic drugs such as docetaxel eliminate MDSC by promoting the differentiation of these cells [34]. In addition, HDACi were previously demonstrated to restore retinoic acid signaling and promote the differentiation of leukemic cells [35]. These data suggest that HDACi may promote MDSC differentiation into mature monocytes, such as macrophages or DC cells. However, further studies are needed to verify these speculations.

In summary, we provided the first evidence that HDACi treatment decreases MDSC accumulation in the spleen, blood and tumor beds and increases the proportion of T cells (particularly that of IFN-γ- or perforin-producing $CD8^+$ T cells) in BALB/C mice with 4T1 mammary tumors. In addition, HDACi exposure of BM cells significantly eliminated the MDSC population induced by GM-CSF or a tumor burden in vitro, which was further demonstrated as functionally important to relieve the inhibitory effect of MDSC-enriched BM cells on T cell proliferation. Mechanistically, the increased apoptosis of $Gr-1^+$ cells compared with that of $Gr-1^-$ cells induced by increasing intracellular ROS via HDACi treatment might at least partially account for the decreased proportion of MDSC observed in the present study. These findings suggest that elimination of MDSC by HDACi treatment may contribute to the overall anti-tumor properties of these cells, highlighting a novel property of HDACi as a potent MDSC-targeting agent, which may be used to enhance the efficacy of immunotherapeutic regimens.

Compliance with ethical standards

Conflict of interest The authors declare no conflicts of interest in the work.

References

1. Gabrilovich DI, Nagaraj S (2009) Myeloid-derived suppressor cells as regulators of the immune system. Nat Rev Immunol 9(3):162–174. doi:10.1038/nri2506

2. Youn J-I, Nagaraj S, Collazo M, Gabrilovich DI (2008) Subsets of myeloid-derived suppressor cells in tumor-bearing mice. J Immunol 181(8):5791–5802. doi:10.4049/jimmunol.181.8.5791

3. Peranzoni E, Zilio S, Marigo I, Dolcetti L, Zanovello P, Mandruzzato S, Bronte V (2010) Myeloid-derived suppressor cell heterogeneity and subset definition. Curr Opin Immunol 22(2):238–244. doi:10.1016/j.coi.2010.01.021

4. Gabrilovich DI, Bronte V, Chen S-H, Colombo MP, Ochoa A, Ostrand-Rosenberg S, Schreiber H (2007) The terminology issue for myeloid-derived suppressor cells. Cancer Res 67(1):425. doi:10.1158/0008-5472.can-06-3037

5. Gallina G, Dolcetti L, Serafini P, Santo CD, Marigo I, Colombo MP, Basso G, Brombacher F, Borrello I, Zanovello P, Bicciato S, Bronte V (2006) Tumors induce a subset of inflammatory monocytes with immunosuppressive activity on $CD8^+$ T cells. J Clin Invest 116(10):2777–2790. doi:10.1172/jci28828

6. Ochoa AC, Zea AH, Hernandez C, Rodriguez PC (2007) Arginase, prostaglandins, and myeloid-derived suppressor cells in renal cell carcinoma. Clin Cancer Res 13(2):721s–726s. doi:10.1158/1078-0432.ccr-06-2197

7. Serafini P, De Santo C, Marigo I, Cingarlini S, Dolcetti L, Gallina G, Zanovello P, Bronte V (2004) Derangement of immune responses by myeloid suppressor cells. Cancer Immunol Immunother 53(2):64–72. doi:10.1007/s00262-003-0443-2

8. Bronte V, Serafini P, Apolloni E, Zanovello P (2001) Tumor-induced immune dysfunctions caused by myeloid suppressor cells. J Immunother 24(6):431–446

9. Marigo I, Dolcetti L, Serafini P, Zanovello P, Bronte V (2008) Tumor-induced tolerance and immune suppression by myeloid derived suppressor cells. Immunol Rev 222(1):162–179. doi:10.1111/j.1600-065X.2008.00602.x

10. Serafini P, Meckel K, Kelso M, Noonan K, Califano J, Koch W, Dolcetti L, Bronte V, Borrello I (2006) Phosphodiesterase-5 inhibition augments endogenous antitumor immunity by reducing myeloid-derived suppressor cell function. J Exp Med 203(12):2691–2702. doi:10.1084/jem.20061104

11. Kodumudi KN, Woan K, Gilvary DL, Sahakian E, Wei S, Djeu JY (2010) A novel chemoimmunomodulating property of docetaxel: suppression of myeloid-derived suppressor cells in tumor bearers. Clin Cancer Res 16(18):4583–4594. doi:10.1158/1078-0432.ccr-10-0733

12. Alizadeh D, Trad M, Hanke NT, Larmonier CB, Janikashvili N, Bonnotte B, Katsanis E, Larmonier N (2014) Doxorubicin eliminates myeloid-derived suppressor cells and enhances the efficacy of adoptive T-cell transfer in breast cancer. Cancer Res 74(1):104–118. doi:10.1158/0008-5472.can-13-1545

13. Suzuki E, Kapoor V, Jassar AS, Kaiser LR, Albelda SM (2005) Gemcitabine selectively eliminates splenic $Gr-1^+$/$CD11b^+$ myeloid suppressor cells in tumor-bearing animals and enhances antitumor immune activity. Clin Cancer Res 11(18):6713–6721. doi:10.1158/1078-0432.ccr-05-0883

14. Vincent J, Mignot G, Chalmin F, Ladoire S, Bruchard M, Chevriaux A, Martin F, Apetoh L, Rébé C, Ghiringhelli F (2010) 5-Fluorouracil selectively kills tumor-associated myeloid-derived suppressor cells resulting in enhanced T cell-dependent antitumor immunity. Cancer Res 70(8):3052–3061. doi:10.1158/0008-5472.can-09-3690

15. Khan AN, Gregorie C, Tomasi T (2008) Histone deacetylase inhibitors induce TAP, LMP, Tapasin genes and MHC class I antigen presentation by melanoma cells. Cancer Immunol Immunother 57(5):647–654. doi:10.1007/s00262-007-0402-4

16. Marks PA, Richon VM, Breslow R, Rifkind RA (2001) Histone deacetylase inhibitors as new cancer drugs. Curr Opin Oncol 13(6):477–483

17. Bolden JE, Peart MJ, Johnstone RW (2006) Anticancer activities of histone deacetylase inhibitors. Nat Rev Drug Discov 5(9):769–784

18. Maeda T, Towatari M, Kosugi H, Saito H (2000) Up-regulation of costimulatory/adhesion molecules by histone deacetylase inhibitors in acute myeloid leukemia cells. Blood 96(12):3847–3856

19. Magner WJ, Kazim AL, Stewart C, Romano MA, Catalano G, Grande C, Keiser N, Santaniello F, Tomasi TB (2000) Activation of MHC class I, II, and CD40 gene expression by histone deacetylase inhibitors. J Immunol 165(12):7017–7024. doi:10.4049/jimmunol.165.12.7017

20. Lee SY, Huang Z, Kang TH, Soong R-S, Knoff J, Axenfeld E, Wang C, Alvarez RD, Chen C-S, Hung C-F, Wu TC (2013) Histone deacetylase inhibitor AR-42 enhances E7-specific $CD8^+$ T cell-mediated antitumor immunity induced by therapeutic HPV DNA vaccination. J Mol Med 91(10):1221–1231. doi:10.1007/s00109-013-1054-9

21. Bayne LJ, Beatty GL, Jhala N, Clark CE, Rhim AD, Stanger BZ, Vonderheide RH (2012) Tumor-derived granulocyte-macrophage colony-stimulating factor regulates myeloid inflammation and T cell immunity in pancreatic cancer. Cancer Cell 21(6):822–835. doi:10.1016/j.ccr.2012.04.025

22. Otaegui D, Rodríguez-Gascón A, Zubia A, Cossío FP, Pedraz JL (2009) Pharmacokinetics and tissue distribution of Kendine 91, a novel histone deacetylase inhibitor, in mice. Cancer Chemother Pharmacol 64(1):153–159. doi:10.1007/s00280-008-0857-9

23. Egorin JM, Yuan Z-M, Sentz LD, Plaisance K, Eiseman LJ (1999) Plasma pharmacokinetics of butyrate after intravenous administration of sodium butyrate or oral administration of tribu-tyrin or sodium butyrate to mice and rats. Cancer Chemother Pharmacol 43(6):445–453. doi:10.1007/s002800050922

24. Jiang G-M, He Y-W, Fang R, Zhang G, Zeng J, Yi Y-M, Zhang S, Bu X-Z, Cai S-H, Du J (2010) Sodium butyrate down-regu-lation of indoleamine 2,3-dioxygenase at the transcriptional and post-transcriptional levels. Int J Biochem Cell Biol 42(11):1840–1846. doi:10.1016/j.biocel.2010.07.020

25. Jiang G-M, Wang H-S, Zhang F, Zhang K-S, Liu Z-C, Fang R, Wang H, Cai S-H, Du J (2013) Histone deacetylase inhibitor induction of epithelial–mesenchymal transitions via up-regu-lation of Snail facilitates cancer progression. Biochim Biophys Acta 1833(3):663–671. doi:10.1016/j.bbamcr.2012.12.002

26. Dokmanovic M, Marks PA (2005) Prospects: histone deacety-lase inhibitors. J Cell Biochem 96(2):293–304. doi:10.1002/jcb.20532

27. Rosato R, Almenara J, Grant S (2003) The histone deacetylase inhibitor MS-275 promotes differentiation or apoptosis in human leukemia cells through a process regulated by generation of reac-tive oxygen species and induction of p21CIP1/WAF1 1. Cancer Res 63(13):3637–3645

28. Mundy-Bosse BL, Lesinski GB, Jaime-Ramirez AC, Benninger K, Khan M, Kuppusamy P, Guenterberg K, Kondadasula SV, Chaudhury AR, La Perle KM, Kreiner M, Young G, Guttridge DC, Carson WE (2011) Myeloid-derived suppressor cell inhi-bition of the IFN response in tumor-bearing mice. Cancer Res 71(15):5101–5110. doi:10.1158/0008-5472.can-10-2670

29. Ma C, Kapanadze T, Gamrekelashvili J, Manns MP, Korangy F, Greten TF (2012) Anti-Gr-1 antibody depletion fails to eliminate hepatic myeloid-derived suppressor cells in tumor-bearing mice. J Leukoc Biol 92(6):1199–1206. doi:10.1189/jlb.0212059

30. Kusmartsev S, Cheng F, Yu B, Nefedova Y, Sotomayor E, Lush R, Gabrilovich D (2003) All-trans-retinoic acid eliminates imma-ture myeloid cells from tumor-bearing mice and improves the effect of vaccination. Cancer Res 63(15):4441–4449

31. van der Most R, Currie A, Mahendran S, Prosser A, Darabi A, Robinson BS, Nowak A, Lake R (2009) Tumor eradica-tion after cyclophosphamide depends on concurrent deple-tion of regulatory T cells: a role for cycling TNFR2-expressing effector-suppressor T cells in limiting effective chemotherapy. Cancer Immunol Immunother 58(8):1219–1228. doi:10.1007/s00262-008-0628-9

32. Rosborough BR, Castellaneta A, Natarajan S, Thomson AW, Turnquist HR (2012) Histone deacetylase inhibition facilitates GM-CSF-mediated expansion of myeloid-derived suppres-sor cells in vitro and in vivo. J Leukoc Biol 91(5):701–709. doi:10.1189/jlb.0311119

33. Ostrand-Rosenberg S (2010) Myeloid-derived suppressor cells: more mechanisms for inhibiting antitumor immunity. Can-cer Immunol Immunother 59(10):1593–1600. doi:10.1007/s00262-010-0855-8

34. Apetoh L, Ghiringhelli F, Tesniere A, Obeid M, Ortiz C, Cri-ollo A, Mignot G, Maiuri MC, Ullrich E, Saulnier P, Yang H, Amigorena S, Ryffel B, Barrat FJ, Saftig P, Levi F, Lidereau R, Nogues C, Mira J-P, Chompret A, Joulin V, Clavel-Chapelon F, Bourhis J, Andre F, Delaloge S, Tursz T, Kroemer G, Zitvo-gel L (2007) Toll-like receptor 4-dependent contribution of the immune system to anticancer chemotherapy and radiotherapy. Nat Med 13(9):1050–1059

35. Ferrara FF, Fazi F, Bianchini A, Padula F, Gelmetti V, Minucci S, Mancini M, Pelicci PG, Coco FL, Nervi C (2001) Histone dea-cetylase-targeted treatment restores retinoic acid signaling and differentiation in acute myeloid leukemia. Cancer Res 61(1):2–7